

A Redshift $z \approx 5.4$ Lyman- α Emitting Galaxy with Linear Morphology in the GRAPES/UDF Field

James E. Rhoads^{1,2}, Nino Panagia^{1,3}, Rogier A. Windhorst⁴, Sangeeta Malhotra¹, Norbert Pirzkal¹, Chun Xu¹, Louis Gregory Strolger¹, Louis E. Bergeron¹, Emanuele Daddi⁵, Henry C. Ferguson¹, Jonathan P. Gardner⁶, Caryl Gronwall⁷, Zoltan Haiman⁸, Anton Koekemoer¹, Leonidas A. Moustakas¹, Anna Pasquali⁹, Adam Riess¹, Sperello di Serego Alighieri¹⁰, Massimo Stiavelli¹, Zlatan Tsvetanov¹¹, Joel Vernet¹⁰, Jeremy Walsh¹², Hao-Jing Yan¹³

ABSTRACT

We have discovered an extended Lyman- α plume associated with a compact source at redshift $z \approx 5.4$ in slitless spectroscopic data from the Grism ACS Program for Extragalactic Science (GRAPES) project. The spatial extent of the emission is about 6×1.5 kpc ($1 \times 0.25''$). Combining our grism data and the broadband images from the Hubble UltraDeep Field (UDF) images, we find a Lyman- α line flux of $\sim 2.2 \times 10^{-17}$ erg cm⁻² s⁻¹ and surface brightness $\sim 7 \times 10^{-17}$ erg cm⁻² s⁻¹/□''. The UDF images show diffuse continuum emission

¹Space Telescope Science Institute, 3700 San Martin Drive, Baltimore, MD 21218.

²Email: rhoads@stsci.edu

³Affiliated with the Space Telescope Division of the European Space Agency, ESTEC, Noordwijk, the Netherlands

⁴Arizona State University, Dept. of Physics & Astronomy, P.O. Box 871504 Tempe, AZ 85287-1504, USA.

⁵European Southern Observatory, Garching, Germany.

⁶Laboratory for Astronomy and Solar Physics, Code 681, Goddard Space Flight Center, Greenbelt, MD 20771

⁷The Pennsylvania State University, 525 Davey Lab, University Park, PA 16802.

⁸Columbia University, New York, NY.

⁹Institute of Astronomy, ETH Hoenggerberg, CH-8093 Zurich, Switzerland.

¹⁰Osservatorio Astrofisico di Arcetri, Italy.

¹¹NASA Headquarters, Washington, DC

¹²ST-ECF, Garching, Germany.

¹³NASA Jet Propulsion Laboratory.

associated with the Lyman- α plume (hereafter UDF 5225), with at least two embedded knots. The morphology of UDF 5225 is highly suggestive of a galaxy in assembly. It is moreover possible that the prominent Lyman- α emission from this object is due to an active nucleus, and that we are seeing the simultaneous growth through accretion of a galaxy and its central black hole. Followup observations at higher spectral resolution could test this hypothesis.

Subject headings: galaxies: high redshift — galaxies: formation — galaxies: interactions — galaxies: starburst — galaxies: individual (UDF 5225)

1. Introduction

The Grism ACS Program for Extragalactic Science (GRAPES) project is a slitless spectroscopic survey that exploits the potential of the G800L grism on the Hubble Space Telescope’s Advanced Camera for Surveys (ACS) to achieve the most sensitive unbiased spectroscopy yet. GRAPES is targeted in the Hubble UltraDeep Field (UDF) region, to complement the UDF direct images, which are in turn the deepest optical imaging to date (Beckwith et al. 2004). The GRAPES survey, and in particular our data analysis methods, are described in more detail by Pirzkal et al. (2004).

One of the primary scientific goals of GRAPES is to study the luminosity function of Lyman break galaxies using spectroscopically confirmed samples at unprecedented sensitivity, and thereby to constrain the faint end luminosity function slope. We have begun this effort through a targeted look at photometrically selected Lyman break candidates, using both i dropout galaxies from the UDF (Malhotra et al 2004) and V dropout galaxies which we have selected (Rhoads et al. 2004) following the selection criteria outlined by Giavalisco et al. (2004b) in both the the v1.0 GOODS survey data (Giavalisco et al. 2004a) and the UDF. (We refer to ACS and NICMOS filters by names of roughly corresponding ground-based filters: F435W \rightarrow B; F606W \rightarrow V; F775W \rightarrow i; F850LP \rightarrow z; F110W \rightarrow J; and F160W \rightarrow H.) Most of the confirmed Lyman break; objects are spatially compact, with sizes ($< 0.5''$) and morphologies typical for the LBG population. In this *Letter*, we describe the most prominent exception to this pattern we have encountered so far, a V dropout object (designated UDF 5225) that is exceptional in its size, morphology, and spectroscopic properties.

Throughout this paper we use the current concordance cosmology ($H_0 = 71 \text{ km s}^{-1} \text{ Mpc}^{-1}$, $\Omega_M = 0.27$, $\Omega_{total} = 1$; see Spergel et al. 2003). Magnitudes are given on the AB magnitude system, so that magnitude zero corresponds to a flux density $f_\nu = 3.6 \text{ kJy} = 3.6 \times 10^{-20} \text{ erg cm}^{-2} \text{ s}^{-1} \text{ Hz}^{-1}$.

2. Observational Properties of UDF 5225

UDF 5225 has two morphological components (see fig. 1): A compact “core,” which is barely resolved in the ACS data (with full width at half maximum $\approx 0.12''$ in the UDF z filter image, which has a point spread function [PSF] with FWHM $\approx 0.10''$) and an extended “plume” with a size $\sim 1.0'' \times 0.3''$. The $i-z$ colors of the two components are roughly similar, with the core marginally redder (by 0.07 mag in the UDF imaging data). The V band shows a weak but real detection of the core, and a hint of emission from the plume. The near-infrared NICMOS images of the object (PI R. Thompson) show a blue color, $z-J = 0.04$ and $J-H = -0.27$, supporting its identification as a Lyman break object with an intrinsically blue spectrum truncated below Lyman- α by the intergalactic medium.

The size is unusual relative to $z \approx 5$ Lyman break galaxies selected photometrically from the GOODS data (Ferguson et al. 2004), which show a broad peak between $0.1''$ and $0.5''$ (comparable to the minor axis size of UDF 5225) and no galaxies as large as $1''$ (the major axis size of UDF 5225).

The 2D ACS grism spectra of UDF 5225 are shown in fig. 2. They detect UDF 5225 significantly in each of the five epochs analyzed (see Pirzkal et al 2004, and see also Riess et al 2004 for more detail on epoch 0). Our strategy of using many roll angles results in a clean separation of the core and plume spectra for epochs 0–2 (roll angles 117° , 126° , and 134°), while the spectra from the two components are superposed in epochs 3 and 4 (217° and 231°). The spectrum from the northwestern tip of the plume is contaminated by the spectrum of an unrelated, brighter object in the PA 134° data, but otherwise the UDF 5225 spectra are free of significant overlap.

Where the plume’s spectrum can be examined independently of other sources, including the core (i.e. epochs 0, 1, and in part 2), it is dominated by a single strong emission line at $\approx 7800\text{\AA}$. Because this line falls in the i filter bandpass, and the plume is detected in both i and z images, we know that there must also be weak continuum emission from the plume on the red side of the line. The core shows both a break and a line at the same wavelength. When both core and plume component spectra are superposed (epochs 3–4,) their combined line and continuum flux results in a stronger spectroscopic detection. We identify the line and break with Lyman- α , based on their wavelength coincidence in the spectrum of the core and based on the B band nondetection and very weak V band flux of the source. This then implies a redshift $z \approx 5.42$, with an estimated uncertainty $\delta z \approx 0.07$. The object is near the upper end of the redshift range for V dropouts (and approaches the redshift range of i dropouts).

We measured the broad band magnitudes of the core and plume components using

the UDF images. We defined apertures to match the morphology of the core and plume components. These apertures follow isophotes in a version of the UDF i band image smoothed with a $0.14''$ FWHM Gaussian kernel, except at the boundary between the two components. (Note, there is no deep minimum in surface brightness separating the core from the plume). We find for the core $i = 27.94$, $i - z = 0.51$, and $V - i \approx 2.3$ mag, while for the plume we obtain $i = 27.39$ mag, $i - z = 0.45$ mag, and $V - i \sim 3.3$ mag. The $V - i$ colors are consistent with transmission through the Lyman- α forest of photons emitted at $912\text{\AA} < \lambda < 1215\text{\AA}$. For a flat (f_ν constant) continuum, we would expect the Lyman- α forest to attenuate the V band flux by a factor of 14 for a source at redshift $z = 5.4$, based on the formalism of Madau (1995).

Because UDF 5225 is both faint and quite extended, it is near the practical detection limit of the GRAPES data. We therefore combine the UDF imaging data, the NICMOS UDF observations, and the GRAPES redshift to estimate the line flux and equivalent width by fitting the spectral energy distribution (SED). We model the intrinsic spectrum as a power law continuum plus an unresolved Lyman- α emission line, modifying both by the Lyman- α forest transmission calculated under the model by Madau (1995). The $z - J$ and $J - H$ colors are unaffected by Lyman- α emission and Lyman- α forest absorption, so we use them to constrain the intrinsic spectral slope to $\alpha \approx -2.4 \pm 0.3$, where $f_\lambda \propto \lambda^\alpha$. With the slope fixed, the $i - z$ and $V - i$ colors are determined by the line flux and the redshift (which determines how strongly Lyman- α forest absorption affects broad band fluxes). For $z = 5.42 \pm 0.07$, we find a rest frame equivalent width of $70 \pm 30\text{\AA}$ and an observed line flux of $(2.2 \pm 0.8) \times 10^{-17} \text{ erg cm}^{-2} \text{ s}^{-1}$. The range in line flux and equivalent width is primarily determined by the range of acceptable redshifts. Changing the continuum slope within its plausible range has a rather smaller effect on the line flux needed to match the $i - z$ color. The observed line flux corresponds to an approximate surface brightness of $7 \times 10^{-17} \text{ erg cm}^{-2} \text{ s}^{-1} / \square''$.

To test whether the Lyman- α emission in UDF 5225 could be powered by an active galactic nucleus (AGN), we examined the UDF direct images from multiple epochs for variability. We stacked the UDF i and z band data into eight epochs of approximately equal exposure time. We also stacked archival z band imaging from HST program 9352, which is shallower than 1/8 of the UDF data but gives a longer time baseline ($\sim 1\text{yr}$). Subtracting the mean of the UDF stacks from each individual epoch shows no significant residuals at the location of UDF 5225, leading us to conclude that the source is not significantly variable in the UDF data. Unfortunately, at $z \approx 5.4$, any CIV line lies beyond the wavelength coverage of the grism (as do all redder AGN lines), while the NV line is not separable from the Lyman- α line at the resolution of the grism. UDF 5225 is not detected in X-rays, based on the 1.0 Msec Chandra Deep Field South catalog (Giacconi et al. 2002), though given its

high redshift, this does not strongly exclude an AGN: Only one AGN at $z > 5$ has been discovered in the two Chandra deep fields so far (Barger et al. 2002), and an X-ray detection would only be expected for a rest frame hard-band luminosity $> 1.8 \times 10^{43} \text{ erg s}^{-1}$. Higher resolution optical spectra of UDF 5225 could convincingly determine whether or not it harbors an AGN by measuring the velocity width of the Lyman- α emission.

3. Models for UDF 5225

What is the nature of the Lyman- α plume in UDF 5225? The line luminosity and the equivalent width are both broadly similar to those seen in narrowband-selected Lyman- α samples (e.g., Rhoads et al. 2000, Malhotra & Rhoads 2002, Ouchi et al. 2003, Hu et al. 2004). The morphology is reminiscent of radio galaxies (e.g. Windhorst et al 1998), quasar jets, the “Lyman- α blobs” that have been observed at $z \sim 3$ (e.g., Steidel et al. 2000), and some other high redshift galaxies (Pascarelle et al 1996, Bunker et al 2000, Keel et al 2002).

We can consider several possibilities: Recombination nebula powered by *in situ* star formation; light from the core component scattered by either electrons or dust; or a recombination nebula powered by the core.

***In situ* star formation:** Star formation would provide a local source of ionizing photons within the plume. It also produces lower-energy photons that would dominate the rest-UV continuum redward of Lyman- α . The resulting continuum slope is the bluest among the models considered here. The Lyman- α equivalent width for star formation should be $\lesssim 240\text{\AA}$ based on stellar population models at Solar metallicity (Charlot & Fall 1993). While observations of Lyman- α galaxies at $z \approx 4.5$ often show larger values (Malhotra & Rhoads 2002), the presence of stars *in situ* will always reduce the equivalent width relative to recombination models where the ionizing photon source is distant. Star formation allows a greater range of morphologies than do mechanisms powered by AGN light. The presence of distinct condensations and a bend in the plume thus both support the star formation model. A conversion factor of $1M_{\odot}/\text{yr} = 10^{42} \text{ erg s}^{-1}$ is widely used for high redshift Lyman- α emission, and would imply star formation at $\gtrsim 7M_{\odot}/\text{yr}$ in the plume, subject to the standard (but untested) assumptions that the star formation follows a Kennicutt (1983) initial mass function (IMF) and that case B recombination is valid. If we base our estimate instead on the rest frame UV continuum emission at 1425\AA , as measured by the z band image, we find a star formation rate of $\approx 4M_{\odot}/\text{yr}$ for the plume (plus another $2.5M_{\odot}/\text{yr}$ in the core, assuming the core light is not dominated by an active nucleus). Given that the conversion factors for both continuum and line light are substantially uncertain (due to

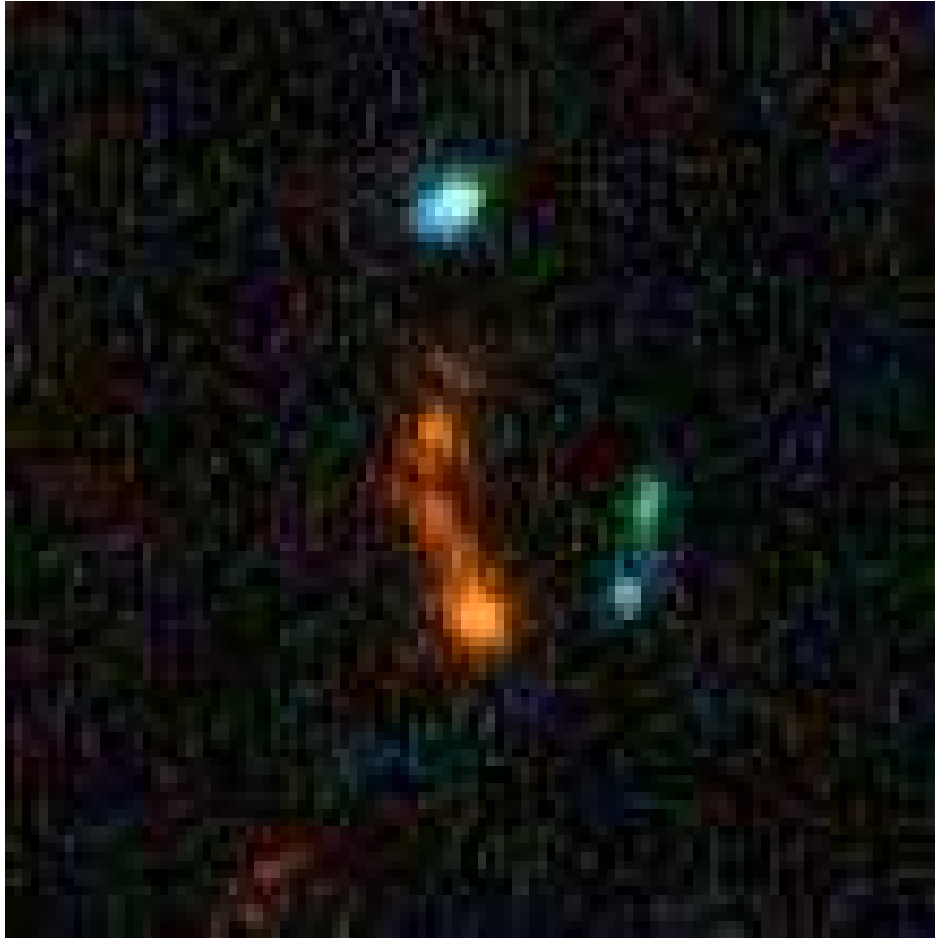


Fig. 1.— Color composite image of UDF 5225 from the Hubble Ultra Deep Field data. The elongated red source in the center is UDF 5225, with the “core” component at the bottom and the plume extending towards the top of the image. The length of the plume is about $1''$. Blue colored objects nearby are unrelated foreground sources. Red represents the z filter, Green an average of V and i, and blue the B filter. Based on the color composite UDF image by Z. G. Levay.

assumptions about the IMF and about the effects of gas and dust on Lyman- α radiative transfer), this constitutes remarkably good agreement.

Scattered Light: If UV radiation from the core encounters a sufficiently dense scattering medium, a detectable scattering cone could be produced. This is the least plausible explanation for the UDF 5225 plume, because the mass in scatterers would have to be unrealistically large for electron scattering, while dust scattering would be unlikely to produce a large Lyman- α equivalent width and a blue continuum color.

We estimate the mass of scattering material required under the approximation that the plume is a cone with length 6kpc and base diameter ~ 2 kpc. The corresponding volume is $2 \times 10^{65} \text{cm}^3$. We estimate the mass for a scattering optical depth τ_e from the core to the end of the cone. Then for electron scattering (with $\sigma_T = 1.6 \times 10^{-24} \text{cm}^2$) we find a number density of $n_e \approx 25\tau_e$ and a corresponding mass of $\sim 5 \times 10^9 \tau_e M_\odot$ in the cone. This gas would emit copious Lyman- α radiation: Indeed, to avoid overproducing the observed Lyman- α luminosity would require that $\tau_e \lesssim 0.025$. Clumping of the scattering gas could further enhance recombinations and further reduce the maximum τ_e for electron scattering to dominate the plume emission.

Such low optical depths imply that electron scattering is a very inefficient way of producing the Lyman- α nebulosity, because scattered light will be suppressed by a factor τ_e . The scattering region must then be illuminated at a much higher intensity than one would naïvely infer from the observed core flux. Consider a simple toy model where the central source has two emission components, one with $\sim 30^\circ$ opening angle that powers the observed plume, and one isotropic that powers the observed core and that we allow to be attenuated by optical depth τ_{abs} of absorption. To reproduce the observed plume to core flux ratio, the collimated component would then need to contain a fraction $\sim 1/[1 + 0.6\tau_e \exp(\tau_{abs})]$, which becomes $\sim 1 - 0.6\tau_e \gtrsim 98\%$ in the limit where $\tau_{abs} \lesssim 1$. This would correspond to a total source UV luminosity $\nu L_\nu \gtrsim 3 \times 10^{45} \text{erg s}^{-1}$ (measured in the z band, which is rest 1410Å) i.e., $7 \times 10^{11} L_\odot$ or an angle-averaged absolute AB magnitude of -23.7 . This luminosity would increase if either the assumed τ_e or degree of collimation were reduced. Such a model would likely require an AGN in the core, because star light cannot be tightly collimated, which would increase the luminosity requirement by another factor of $\gtrsim 10$ while requiring also $\tau_{abs} \gtrsim 2$ on the line of sight to the core. The mass of ionized hydrogen required in an electron scattering scenario would be modest, $\lesssim 10^8 M_\odot$.

Dust scattering in an ionized medium could work, as long as the optical depth is suitably small so that (a) there is no significant reddening of the scattered continuum light, and (b) Ly-a radiation is not selectively absorbed relatively to the continuum. Condition (a)

requires $\tau \lesssim 0.1$ at rest 1300\AA , and similarly condition (b) requires $\tau \lesssim 0.05$ at rest-frame 1216\AA to avoid attenuation of Lyman- α by more than a factor of 2 (Panagia and Ranieri 1973a, b). The associated total mass of gas and dust would be $M_{\text{plume}} \approx 10^7 \tau_{\text{dust}}(1216\text{\AA}) M_{\odot}$ assuming a dust-to-gas mass ratio of 0.01. Inserting $\tau_{\text{dust}} < 0.1$ gives $M_{\text{plume}} \sim 10^6 M_{\odot}$. The requirement on the core luminosity can be derived exactly as for the electron scattering case, but now with larger scattering opacity, so the final constraint becomes $\nu L_{\nu} \gtrsim 3 \times 10^{44} \text{ erg s}^{-1}$.

However, scattered light faces several problems. First, the bend in the plume can only be produced if the apparent geometry is set by the spatial distribution of the scatterers, rather than the geometry of quasar emission. Second, the intensity of scattered light should decrease away from the AGN (falling off as r^{-2} in the simplest case, though projection effects and anisotropic quasar emission could modify this). In contrast, the strongest knot in the plume is at the largest projected separation from the core.

Recombination powered by core light: This model is like the electron scattering model but for higher densities, where recombinations become more important than electron scattering. In this case the mass of ionized hydrogen involved would be $\gtrsim 10^8 M_{\odot}$. The core luminosity could be much lower in this case: For an ionization bounded nebula, it need only be about twice the measured Lyman- α luminosity, i.e., $> 2 \times 10^{43} \text{ erg s}^{-1}$ in ionizing radiation, although it could be much larger if the radiation is largely isotropic and the morphology of the plume is set by where there is substantial gas.

However, in this case, the continuum emission from the plume would be pure nebular emission, with components from the two-photon process, bound-free emission, and free-free emission. The expected equivalent width of the line would then be $> 1000\text{\AA}$ (rest frame) and the z band continuum should be much weaker than we see. While dust attenuation of the Lyman- α might help, the model would have to be fairly contrived to simultaneously fit the Lyman- α flux, continuum flux, equivalent width, and color in the plume, and we therefore disfavor this model also. The only countervailing argument comes from the V band flux, which should be absent in a two-photon continuum and is indeed rather weaker in the plume than the core. However none of the V band detections are strong, so it is not clear if the difference in $V - i$ and $V - z$ colors between the two components is significant.

A Merger Scenario: Consider a merger scenario for UDF 5225, where the morphology indicates a major merger in progress at $z = 5.4$. The nuclei of the two interacting galaxies would then presumably be the “core” component we have discussed plus the brightest “knot” in the plume, which lies a full arcsecond away. The projected separation, $\sim 6\text{kpc}$, would then imply a crossing time of order $60v_{100}\text{Myr}$, where v_{100} is the relative velocity of the two

components in units of 100 km s^{-1} . Multiplying this by the star formation rates inferred in section 3 implies formation of some few $\times 10^8 M_{\odot}$ of stars in the course of the interaction.

The star formation rate per unit area, based conservatively on the UV-derived SFR for the plume, is $\sim 0.4 M_{\odot} \text{ yr}^{-1} \text{ kpc}^{-2}$. Comparing to the global Schmidt law for star formation, we would infer a gas mass surface density of $\sim 800 M_{\odot} \text{ pc}^{-2}$, for a total gas mass of order $7 \times 10^9 M_{\odot}$. This number implies a gas consumption time scale of $\sim 10 t_{\text{dyn}} \sim 600 \text{ Myr}$, though if star formation is proceeding at an atypically high rate (driven by interaction), the gas reservoir could be smaller.

4. Discussion

We have examined several possible models for the observed properties of the galaxy UDF 5225, a very faint and high redshift object with a core-plume morphology and prominent Lyman- α emission. We conclude that the Lyman- α emission is most likely powered by *in situ* star formation throughout the galaxy. Present evidence neither requires nor rules out the presence of an AGN in the core component. Followup spectroscopy using higher spectral resolution and/or coverage into the near infrared would provide new information that could settle the AGN question. However there seems to be no compelling need for an AGN component to explain the observed UV and Lyman- α emission. Rather, tidally triggered star formation in a merging galaxy pair seems to describe the galaxy well. As such, it may be a particularly spectacular example of the broad class of star-forming Lyman break galaxies that dominate the galaxy population observed in the Hubble Ultra Deep Field and other very sensitive, high redshift galaxy surveys.

We thank the STScI Director and the UDF team for their hard work in designing and executing the UDF experiment. We thank Zoltan G. Levay for producing the color composite shown in figure 1. This work has been supported under grant number HST-GO-09793. C.G. acknowledges support from NSF-AST-0137927. L.A.M. acknowledges support by NASA through contract number 1224666 issued by the Jet Propulsion Laboratory, California Institute of Technology under NASA contract 1407.

REFERENCES

- Barger, A. J., Cowie, L. L., Brandt, W. N., Capak, P., Garmire, G. P., Hornschemeier, A. E., Steffen, A. T., & Wehner, E. H. 2002, AJ 124, 1839

- Beckwith, S. V. W., et al. 2004, in preparation
- Bunker et al 2000, ApJ 531, 95
- Charlot, S., & Fall, S. M. 1993, ApJ 415, 580
- Ferguson, H. C., et al. 2004, ApJ 600, L107
- Giacconi, R. et al. 2002, ApJS 139, 369
- Giavalisco, M., et al. 2004a, ApJ 600, L93
- Giavalisco, M., et al. 2004b, ApJ 600, L103
- Hu, E. M., Cowie, L. L., Capak, P., McMahon, R. G., Hayashino, T., & Komiyama, Y. 2004, AJ 127, 563
- Keel, W. C., Cohen, S. H., Windhorst, R. A., & Waddington, I. 1999, AJ 118, 2547
- Kennicutt, R. C., Jr. 1983, ApJ 272, 54
- Madau, P. 1995, ApJ 441, 18
- Malhotra, S., & Rhoads, J. E. 2002, ApJ 565, L71
- Malhotra, S., et al. 2004, in preparation
- Ouchi, M., et al. 2003, ApJ 582, 60
- Panagia, N., & Ranieri, M. 1973a, A&A 24, 219
- Panagia, N., & Ranieri, M. 1973b, Mem. Soc. Roy. Sci. Liège, 6 série, tome V, 275-280.
- Pascarelle, S. M., Windhorst, R. A., Keel, W. C., & Odewahn, S. C. 1996, Nature 383, 45
- Pirzkal, N. et al. 2004, ApJ submitted; astro-ph/0403458
- Rhoads, J. E., Malhotra, S., Dey, A., Stern, D., Spinrad, H., & Jannuzi, B. T. 2000, ApJ 545, L85
- Rhoads, J. E., et al. 2004, in preparation
- Riess, A., et al. 2004, ApJ 600, L163
- Spergel, D. N., et al. 2003, ApJS, 148, 175
- Steidel, C. C., Adelberger, K. L., Shapley, A. E., Pettini, M., Dickinson, M., & Giavalisco, M. 2000, ApJ 532, 170
- Windhorst, R. A., Keel, W. C., & Pascarelle, S. M. 1998, ApJ 494, L27

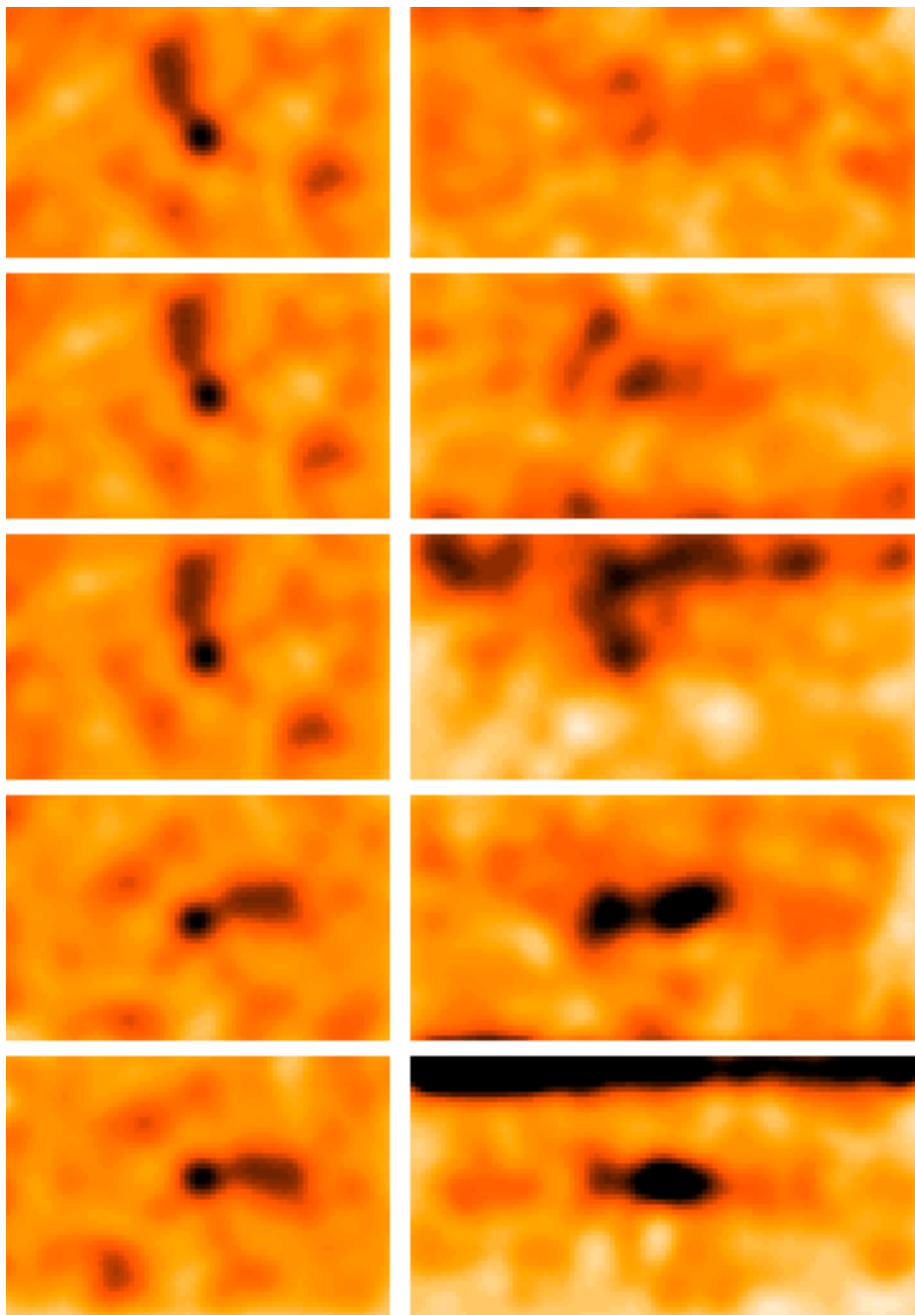


Fig. 2.— The GOODS survey v1.0 direct image of UDF 5225 in the z' (F850LP) filter (left panels), together with the 2-D GRAPES spectra at each of five roll angles (right panels). From top to bottom, the angles shown are PA 117, 126, 134, 217, and 231°. The direct image is the same in all rows but is rotated to match the roll angle of each 2D grism spectrum cutout. All images have been smoothed with a Gaussian filter matched to the angular size of the plume component (0.3" FWHM) for maximum clarity. The upper edge of the grism spectrum in the third PA shows contamination by an unrelated source elsewhere in the image. The Lyman- α emission from both plume and core is most clearly visible in the second and third panels; the first panel is at a similar roll angle but is shallower. In the fourth and fifth panels, the line emission from the plume falls atop continuum emission from the core, resulting in a higher surface brightness in the dispersed image.